論文 / 著書情報
Article / Book Information

Title	Long-Term Design of Mangrove Landfills as an Effective Tide Attenuator under Relative Sea-Level Rise
Authors	Hiroshi Takagi
Citation	Sustainability, Vol. 10, 4
Pub. date	2018, 4
Creative Commons	Information is in the article.

sustainability

MDPI

Article

Long-Term Design of Mangrove Landfills as an Effective Tide Attenuator under Relative Sea-Level Rise

Hiroshi Takagi

School of Environment and Society, Tokyo Institute of Technology, Tokyo 152-8550, Japan; takagi@ide.titech.ac.jp

Received: 4 February 2018; Accepted: 28 March 2018; Published: 2 April 2018

Abstract: A mangrove ecosystem is an important option in Ecosystem based Disaster Risk Reduction (Eco-DRR). The effectiveness of an artificial mangrove landfill in reducing tidal amplitudes was studied by performing a coupled numerical model that simulated wave propagation and soil consolidation. The constructed model simulated the propagation of tide over an artificial landfill that was subjected to land subsidence, sea-level rise, vegetation growth, and sediment deposition. A case study analysis confirmed that the tidal amplitudes are reduced if the initial elevation of the landfill is appropriately considered to achieve an equilibrium state of the landfill over its lifetime. Sediment deposition may be the only dependable source to sustain the surface elevation of a mangrove with relative sea-level rise. Sediment deposition is important to promote vegetation growth, which in turn contributes to sedimentation by enhancing a tranquil hydrodynamic environment. An insufficient initial elevation of the landfill will result in less effective protection against tidal propagation after it substantially subsides.

Keywords: mangrove landfill; land subsidence; sea-level rise; ocean tides; numerical model

1. Introduction

Mangrove forests and their artificial landfills are expected to act as natural buffers against hydrodynamic disturbances such as ocean tides, high waves, tsunamis, and storm surges. Coastal flooding could be reduced by constructing a mangrove plantation zone, which will cause a reduction in flow velocity and an increase in flow smoothing effects [1]. Vegetation also mitigates wave impacts as the density and diameter of plants increase. Salt marshes are expected to contribute to the reduction in wave loads on coastal dikes [2,3]. Mangroves also increase the resilience of a shoreline by providing ecosystem services such as sediment traps, flood mitigation, wildlife habitats, nutrient recyclers, and nurseries [4,5]. The benefits of mangroves are referred to as *ecological resilience*. An ecological system absorbs hydrodynamic turbulence and reorganizes the system in a way that retains the function and structure of ecosystem feedbacks [6,7]. The function of mangroves has drawn worldwide attention as an Ecosystem-based Disaster Risk Reduction (Eco-DRR). Eco-DRR is defined as the "sustainable management, conservation and restoration of ecosystems to reduce disaster risk, with the aim to achieve sustainable and resilient development". The appropriate management of ecosystems is expected to reduce disaster risk as well as climatic risks [8–10]. However, the effectiveness of an ecosystem in reducing hydrodynamic impacts needs to be evaluated to realize appropriate the Eco-DRR response. For example, despite enormous funds being dedicated to the planting of mangrove forests over recent decades in the Philippines, the survival rates of mangroves are only 10–20% [4].

This study investigates the application of mangrove forests on a landfill (hereinafter referred to as the mangrove landfill) as a countermeasure for reducing tidal influence in urban areas, which are undergoing a rapid land subsidence. For instance, Jakarta is one of the fastest growing cities

in the world and it has been experiencing subsidence rates, which have exacerbated the coastal flooding issues [11]. Coastal dikes in Jakarta will help to prevent flooding for a while. However, their effectiveness will shortly disappear if land subsidence does not stop [12]. Some small island communities in the Philippines were subjected to frequent coastal flooding due to a sudden land subsidence triggered by the Bohol earthquake in 2013 [13]. Intense groundwater use, as well as natural consolidation, accelerated the rate of the subsidence in the Chao Phraya Delta, Thailand, and the Mekong Delta, Vietnam, which reached 5–15 cm/year and 2 cm/year, respectively [14,15]. On the other hand, the sediment accretion in mangrove forests is relatively slow, with a rate of several mm/year [16,17]. Therefore, the surface elevation of mangrove forests are unlikely to keep pace with current IPCC sea-level rise scenarios [18]. The response of a mangrove system to external influences (e.g., sea-level rise and land subsidence) determines the capacity of a forest to maintain itself at the rate necessary to adapt to relative sea-level rise. Constructing a mangrove landfill without considering such subsidence will end up with the forest's submergence in a short period of the time. For instance, the mangrove landfill attached to a Jakarta's Fishery Port worked as an effective mangrove landfill, protecting the port against waves [19]. However, it has been sinking over the last decade, and the ground elevation has now become below mean sea level (Figure 1). An engineering design that considers land subsidence and sea-level rise is necessary to assist planners when applying a mangrove landfill as an Eco-DRR option in urban areas.

This study evaluates tidal propagations over mangrove landfills to quantify the effectiveness of mangroves in attenuating their amplitudes, with particular emphasis on the long-term evolution associated with sea-level rise, land subsidence, vegetation growth, and sediment deposition.

Figure 1. The mangrove landfill works to protect the Jakarta Fishery Port from waves. However, it is sinking due to a land subsidence (Photo taken in Feb 2016).

2. Methodology

The concept of the mangrove landfill is described. A model that simulates tidal propagation on a sinking landfill is then explained. Finally, the numerical conditions are described to investigate the applicability of the proposed method to a particular situation.

2.1. The Mangrove Landfill Concept

Urban coastal areas are experiencing increases in disaster risks, exacerbated by many challenging issues such as sea-level rise, rapid population increase, land subsidence, and an aging infrastructure. Ecosystem landfills are expected to mitigate such disaster risks. Figure 2 illustrates the concept of such a system, showing two distinctive scenarios: (a) extensive inundation induced by a high tide resulting in the overflowing of a coastal dike and (b) a mangrove landfill system adopted to reduce flood impacts.

In the beginning of the first stage of (b) (Scenario 1), a front section of the landfill is shaped into a trapezoidal form by filling soil. In this stage, the landfill acts as an ordinary dike structure because the ground surface is sufficiently higher than the tidal levels. However, the landfill will soon start sinking due to soil consolidation resulting from its own weight and/or the regional land subsidence. Therefore, two future scenarios are also illustrated: Scenario 2 shows the scenario where the landfill is maintained with sea-level rise as a result of an equilibrium state among subsidence, sea-level rise, and sediment deposition. On the other hand, Scenario 3 represents that landfill designed without due consideration about the long-term evolutions that will be submerged under sea level. In this state, mangrove plantations cannot grow anymore because strong waves propagate over the mangrove landfill without reduction, causing less sediment trap and no remarkable effect on the tidal attenuation in turn. Scenario 4 shows another scenario where the landfill is constantly higher than sea level during its lifetime, which could happen when the initial elevation of the landfill is set high enough or the soil does not undergo consolidation. In this situation mangroves cannot grow if the ground is positioned above high tide level, while some terrestrial plants may still cover the surface. Although Scenario 4 may not be conceived of as an Eco-DRR option, it also works as a hard countermeasure in mitigating coastal flooding.

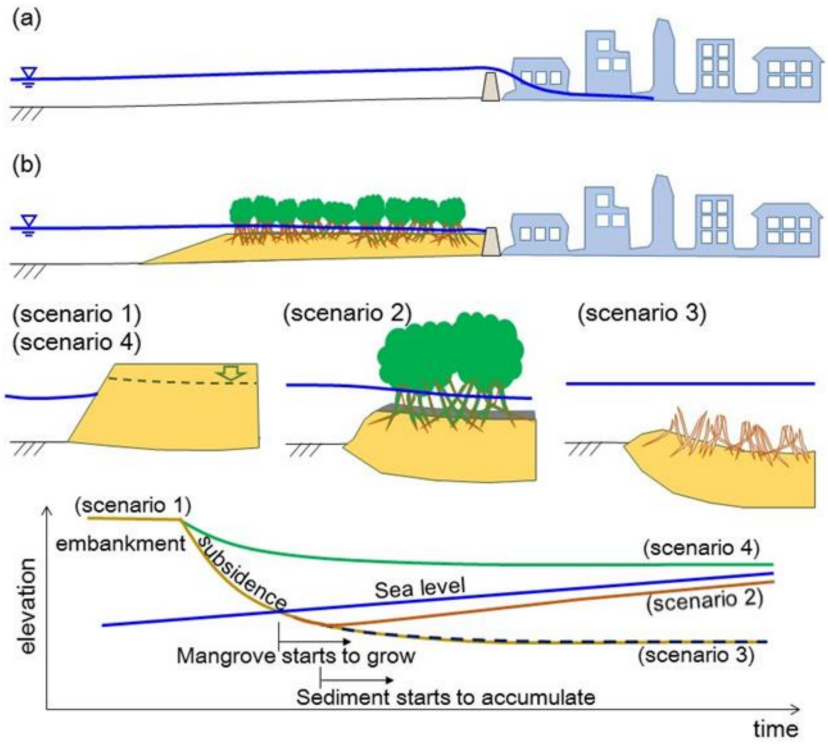

Figure 2. Artificial mangrove-covered landfills and their transitions over time: (Scenario 1) initial cross-section of the landfill; (2) land subsidence is balanced with the rate of sea-level rise; (3) land subsidence is excessive, and thus tides are not reduced; and (4) land subsidence is slow, and the surface is not submerged within the lifetime.

2.2. Long Wave-Consolidation Coupled Modelling

Figure 3 shows the scope of the proposed model. This study only focuses on tide-induced floods. In order to assess the effectiveness of mangrove landfills to mitigate coastal floods, the present study has chosen the tides as the most influential driver of the floods. Tides are categorized as long-period waves, which have a wave length far greater than the water depth. The range of long-period waves is typically 5 min to 12 h, ranging from tsunamis to astronomical tides [20]. Floods can also be caused by other mechanisms, such as tsunamis and storm surges. However, tides are the longest among

those categorized as long waves. Generally, the longer the wave length, the less the energy dissipates. Therefore, tides can be considered the most persistent oceanic phenomenon that induce coastal floods.

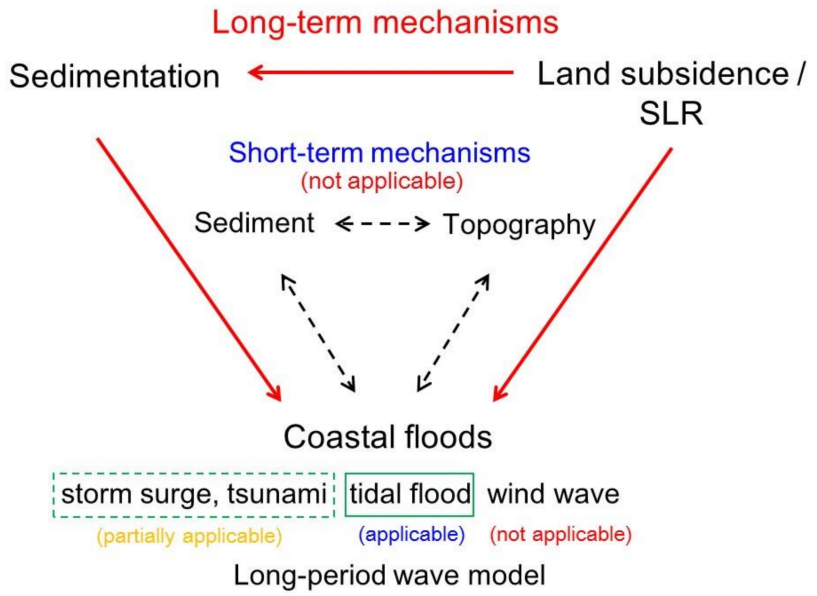

Figure 3. The scope, applicability, and limitation of the proposed long wave-consolidation coupled model.

Long waves could be simulated by solving the two equations: the continuity equation, Equation (1) and the equation of motion, Equation (2) e.g., [21,22]:

$$\frac{\partial \eta}{\partial t} + \frac{\partial (h_i + \eta)\overline{U}}{\partial x} = 0 \tag{1}$$

$$\frac{\partial \overline{U}}{\partial t} + \overline{U}\frac{\partial \overline{U}}{\partial x} + g\frac{\partial \eta}{\partial x} + \frac{gn^2|\overline{U}|\overline{U}}{h_i^{4/3}} = 0 \tag{2}$$

η is water surface elevation from the still water level, $\overline{U}$ is depth-averaged velocity, h_i is water depth at the ith year, n is Manning's n, and g is gravitational acceleration. These equations were discretized by FDM (the finite difference method) with staggered grids, in which water surface node and velocity node are shifted half a grid point to each other. The staggered grid is known to prevent numerical oscillations that may be excited on the non-staggered grid. The derivatives of the temporal terms are approximated by the forward difference method, while the spatial derivatives are discretized by the central differences. A sinusoidal wave and wall boundary conditions are assigned at the offshore and onshore computational boundaries, respectively. The former boundary reproduces the fluctuation of tides, while the latter one represents a vertical coastal dike dividing the mangrove landfill from a community behind the dike, as shown in Figure 2b.

Equations (1) and (2) are equivalent with Saint-Venant equations, in which discharge Q is commonly used instead of depth-averaged velocity. Note that these equations have been derived for non-zero water-depth conditions, and therefore they are no more valid when the water depth becomes zero or a negative value. An inclusion of the algorithm referred to as "drying and wetting scheme" is expected to improve the representation of rapidly varying flows as a result of sudden water changes. However, the simulation of water waves is particularly challenging near dry areas. The standard numerical methods may fail at the dry/wet fronts and produce negative water heights [23]. However, it is obvious that the landfills of their surfaces immediately closed to the water surface appears to be more effective in reducing tidal influences than those that are fully inundated. Thus, the present model

did not incorporate any dry/wet schemes. Instead, in this model moderate water depths (i.e., not too shallow) are assumed in order not to cause an instability of computation.

The relative depth (the water depth divided by the wave length) is often used to classify the types of waves. If the relative depth is shallower than 1/20, the wave can be classified as a long-period wave [24]. The long-wave assumption is almost completely justified for ocean tides even in very deep sea. Not only ocean tides but also tsunamis and storm surges are considered as long-period waves [20,22]. Unlike tides, however, relatively rapid changes in water level may cause non-linear phenomena, such as bore or soliton fission during tsunamis or storm surges [25]. Because mangrove inhabits very shallow regions, these complex characteristics will be particularly pronounced. Thus, the depth-averaged assumption adopted in the equations cannot be applicable if such a mechanism is not negligible. On the other hand, it is obvious that wind waves of periods less than 15 s are by no means long-period waves, and thus it is not appropriate to apply the proposed model to ordinary waves.

An increase in stress gradually causes a reduction in soil volume as water is released from it, resulting in *consolidation*. This term is not the same as *compaction*, which is an instantaneous change in soil volume because of a mechanical load. In the long wave soil consolidation coupled model developed, the water depth used in Equations (1) and (2) varies in accordance with the one-dimensional consolidation over time t that can be calculated by the Terzaghi consolidation equation as follows e.g., [26,27]:

$$\frac{\partial u_e}{\partial t} = C_v \frac{\partial^2 u_e}{\partial z^2} \tag{3}$$

u_e is the excess pore pressure in soil, C_v is the consolidation coefficient, and z is the vertical ordinate.

A non-dimensional form of Equation (3) can be derived as follows:

$$\frac{\partial u_e}{\partial \bar{t}} = \frac{\partial^2 u_e}{\partial \bar{z}^2} \tag{4}$$

where, $\bar{z} = z/H_d$ and $\bar{t} = C_v t/H_d^2$. H_d is the length of drainage path, which is a half of the layer thickness (in the case drainage occurs at both top and bottom boundaries) or the full layer thickness (drainage only occurs at one boundary, either top or bottom). Equation (4) can be solved with boundary and initial conditions. The approximate solution is derived by applying the initial condition of the excess pore pressure u_e, which is calculated based on the landfill load of q_s as follows:

$$u_e = q_s \sum_{n=0}^{\infty} \frac{2(-1)^n \cos(a_n \bar{z})}{a_n} \exp\left(-a_n^2 \bar{t}\right) \text{ where, } a_n = (2n+1)\pi/2 \tag{5}$$

The final displacement is then estimated by Equation (6). C_c is compression index. The subsidence at a given time, S_c, can be calculated by Equations (7) and (8) by applying the consolidation degree U. In the proposed model, the effective stress σ' in Equation (6) is calculated based on Osterberg's method for vertical stress induced by landfill loads [28].

$$S_f = \frac{C_c}{1+e_0} H log_{10}\left(1 + \frac{q_s}{\sigma'}\right) \tag{6}$$

$$S_c = S_f U(\bar{t}) \tag{7}$$

$$U(\bar{t}) = \int_0^1 \left(1 - \frac{u_e}{q_s}\right) d\bar{z} = 1 - \sum_{n=0}^{\infty} \frac{2}{a_n^2} \exp\left(-a_n^2 \bar{t}\right) \tag{8}$$

In the end, the water depth h_i in the long-period wave model (Equations (1) and (2)) can be updated by considering the estimated subsidence. In addition, the sea-level rise and sediment deposition should also be incorporated in determining the resultant water depths above the surface of the mangrove landfill.

Figure 3 also conceptualizes a complex interaction mechanism among currents, waves, and sedimentation that cause topographical variations. Many sediment transport equations have been proposed over the last several decades. Among them, the Einstein model [29] and the Bagnold model [30] are two predominant equations when calculating sediment transport rates as a form of *bedload*, which is a particle movement that is rolled or dragged in a stream. This causes a cross-shore evolution that occurs in a shorter time scale, such as a seasonal cycle [31]. However, the selection of appropriate equations is still not clear because of difficulties in conducting measurements of sediment transport [32]. Although these short-term mechanisms appear to be important in determining the topography of the mangrove landfill, this study only investigated the cycles of the long-term mechanisms, as presented in Figure 3.

2.3. Resistance of the Mangrove System

Tidal flows are subjected to the resistance of the mangrove vegetation. Such resistance is composed of two driving factors: energy losses due to drag force and friction [33,34]. Drag related to the Reynolds number, diameter, plant height, and vegetation density have been investigated by many previous studies [35–37]. However, the present long wave model only can evaluate bottom friction, which is considered via Manning's n value. While coastal areas without dense vegetation are assumed to take a relatively small n value [38], a greater value needs to be selected where the flow is simulated in a dense vegetation area. Table 1 summarizes the Manning's values used in some previous studies, demonstrating that the values substantially change depending on conditions. This study assumes the n value to be 0.3 in Equation (1) to take into account a fully-grown state of mangrove vegetation, as a result of averaging all those listed in the table. It should be noted that the n value for an initial bare landfill (condition without a mangrove) was taken at a smaller value of 0.025, which is often assumed as the roughness of the seabed [38].

Table 1. Manning's values depending on vegetation conditions.

Manning's n Value (s m$^{-1/3}$)	Event	Test Location	Vegetation Type	References
0.2–0.4	Tide	Coral Creek, Queensland, Australia	Mangrove	Wolanski et al. (1980) [39]
0.1–0.2	Flood	Various flood plains in the US	Dense bushy willow, etc.	Arcement and Schneider (1984) [40]
0.2–0.7	Tide	Nakama-Gawa, Okinawa, Japan	Mangrove	Mazda et al. (1997) [35]
0.1	Tide	Middle Creek, Cairns, Australia	Mangrove	Furukawa et al. (1997) [41]
0.15	Storm surge	South Florida, US	Mangrove	Xu et al. (2010) [42]
0.075–0.505	Field channel test	Guadalajara, Castilla la Mancha, Spain	Grassland, Scrubland, Pine forest	Diaz (2005) [43]

2.4. Rate of Sediment Trap

In their natural condition mangroves respond to relative sea-level rise and thus artificial maintenance is not required. A sediment trap naturally occurs in wetlands because of the deposition of organic matters yielded by the plants themselves [44]. Many previous investigations suggest that coastal marshes accrete at rates comparable to sea-level rise e.g., [45–49]. For example, an organic deposition of 9 mm/year was recorded in a marsh covered by *Spartina alterniflora* [50]. An extensive two-year field observation in a mangrove swamp found that the deposition rate was an average of 10.6 mm/year [51]. In this way, mangroves could work as a trap for suspended sediment [52]. It is obvious that the deposition rate significantly changes depending on various environmental conditions. Sedimentation trapped by the mangrove also depends on whether the plant grows fully or partially. However, the following case study simplified that sediment deposition constantly takes place at the rate of 10 mm/year, given those rates in the previous studies. This deposition will increase the load q_s

in Equation (5), resulting in an acceleration of subsidence. In a more detailed analysis, various types of substances in addition to soil should also be considered, which include shells, dead marine organisms, and even trash, such as shown in Figure 1.

2.5. Conditions Assumed in the Case Study

A case study analysis was performed to investigate how tides attenuate across the mangrove landfill. In this analysis, various parameters were determined by referencing to the previous studies, investigating land subsidence, coastal floods, and mangroves in the Jakarta Bay [1,11,12]. Numerical settings and other assumptions are summarized as listed in Table 2. The analysis was performed only for a diurnal-tide condition to simply conceptualize the problems and to examine for an unfavorable condition, in which the mangrove does not effectively work as a tidal attenuator. Long-wave attenuation becomes more pronounced as the flow velocity increases. If their amplitudes are the same, semi-diurnal tides appears to be more attenuated than diurnal tides. Therefore, diurnal-tide component is ideal in investigating the effectiveness of the mangrove landfill. The proposed model assumes the vegetation growth ratio, which represents to what extent the mangrove can resist tidal current, in order to incorporate the influence of the plant density. This ratio is hypothesized as a linear growth from 0% at first and reaches up to 100% 10 years later.

Table 2. Various conditions in the case study analysis.

Factor	Setting/Condition
Time span of the analysis	100 years after the completion of the landfill.
Spatial grid	50 m × 600 computational grids = 30 km in the cross-shore direction.
Original bathymetry	Varying from a 10-m depth offshore to a 1.5-m depth onshore; the mangrove embankment is created on top of the original bathymetry.
Embankment heights (thicknesses)	2, 3, 4 and 5 m
Time increment for shallow water wave computation	0.2 s
Boundary condition	Offshore: A diurnal tide with amplitude of 0.3 m, imposed as a sinusoidal wave. Onshore: Wall boundary condition (i.e., $U = 0$ at the end of the computational domain).
Computational time	24 h, which can fully encompass one tidal cycle.
Sediment accretion	Accretion on the embankment will start after the mangrove plants are fully grown.
Mangrove plants	Plants will be fully grown in 10 years.
Bottom roughness	Manning's n will linearly increase from the initial value of 0.025 (the embankment not covered by vegetation) to the final value of 0.30 (fully covered by vegetation) over the growing period.
Soil consolidation parameters	$C_c = 1.0$; $C_v = 85.0$ cm^2 day^{-1}
Soil consolidation layer	A mangrove embankment filled with sand (unit weight of 21 kN m^{-3}) is to be placed on top of the clay seabed layer (unit weight of 18 kN m^{-3}); the consolidation process occurs only in the clay layer, of which the thickness is assumed to be 18.5 m (from −1.5 m down to −20 m below still-water level).
Sea-level rise	Sea level will continue to rise at the rate of 7 mm year^{-1}

3. Results

The effectiveness of the mangrove landfill in reducing tidal amplitude is discussed based on the case analysis.

3.1. Ground Elevation over the Lifetime and Tidal Attenuation on the Mangrove Landfill

In the case study, the original bathymetry was assumed to be constant with the water depth of 1.5 m, as shown in Figure 4a. The mangrove landfill was constructed on the basement. Two initial elevations were tested: a high mound with a thickness of 5 m and a low mound with a thickness of 2 m, as illustrated in Figure 4b. Figure 4c projects that both scenarios eventually become submerged 60 years later. However, the surface retained its position close to the sea surface elevation when the thickness was 5 m. In the case of the 2 m thickness, however, the water depth became about 1.5 m, which is the same as the pre-filling condition. This implies that a sufficiently high landfill may work

as a countermeasure over its lifetime, whereas the function of a low-elevation landfill will be shortly degraded, completely losing the functionality after a few decades.

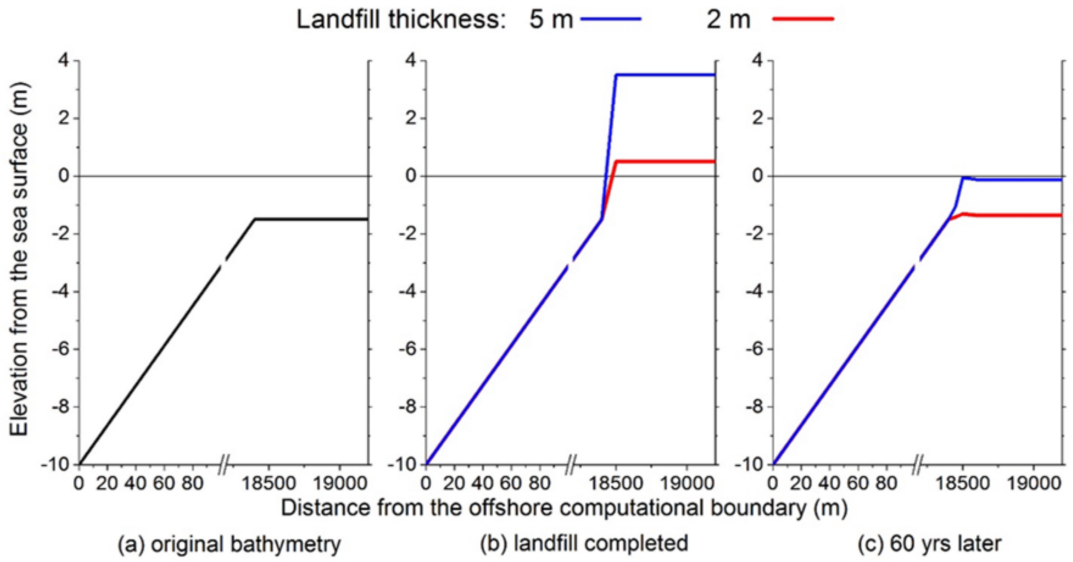

Figure 4. Transitions of mangrove landfills for two different landfill conditions.

Changes in the ground level will inevitably differ with and without sediment trap over time (Figure 5). The difference is obvious, particularly for the 5 m landfill case. Sediment deposition is not yet calculated in the first four decades because the ground level remains above the sea surface. After five decades, the landfill surface starts to be inundated. The landfill with receiving sediment deposition is expected to maintain with the relative sea-level rise, showing a successful case. Contrarily, the lower landfill's case may not contribute to a reduction in tidal amplitudes because the water depth is too deep to effectively mitigate the energy of the incoming tide. The geometric parameters of the landfill, such as height and width, appear to be predominant factors on tidal attenuation.

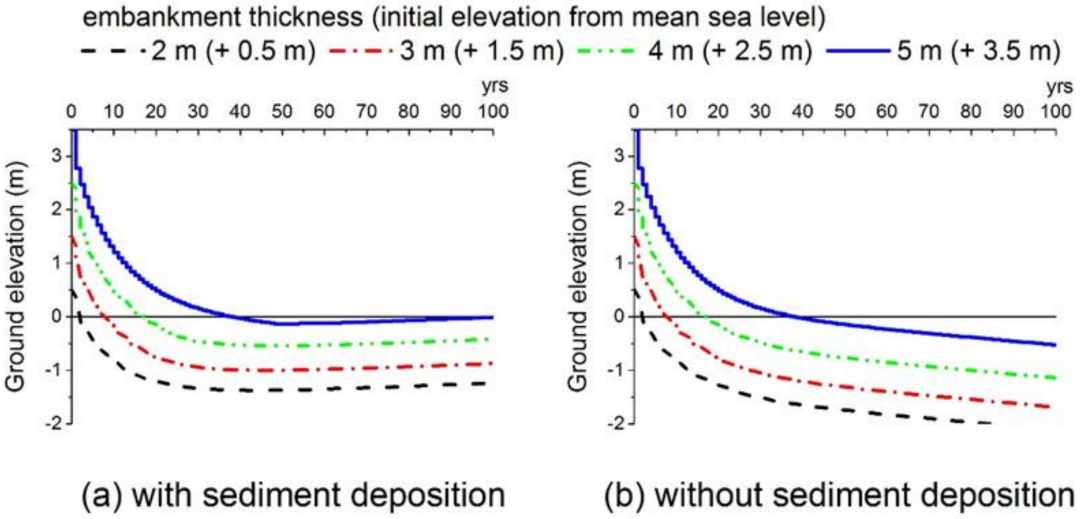

Figure 5. Ground level changes over the century: (**a**) with deposition; (**b**) without deposition. The elevations are monitored at 19,000 m in Figure 4 (i.e., 500 m inland from the landfill's shoulder).

Figure 6 demonstrates how the effectiveness of a tidal attenuator would vary with changes in the parameters of the mangrove landfill. The amplitude of the tide does not remarkably decrease

when the growth ratio is relatively low. For instance, it is found that tide is not attenuated when no vegetation covers the landfill in the case of water depth with 1 m. On the other hand, if the landfill is constructed to be as wide as 500 m and the plants are fully grown, the reduction in amplitude reaches about 40%. If the water depth can be kept shallower than 50 cm, the landfill width can be shrunk by 200 m, resulting in a sufficient amplitude reduction of 40 to 50%.

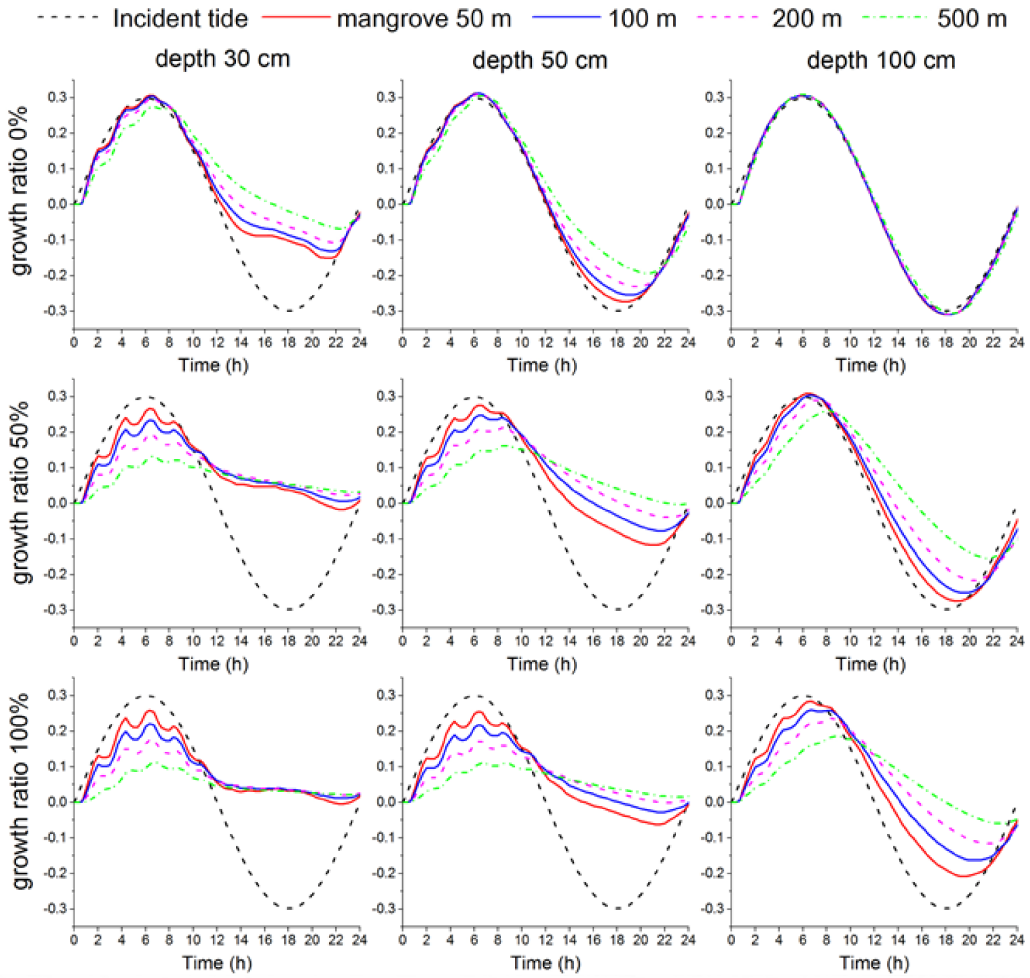

Figure 6. Tidal amplitudes over the mangrove landfills with four different widths. The vertical axis shows water-surface elevation (unit: meters), while the horizontal axis indicates the time from the beginning of the computation (unit: hour).

Figure 6 also shows that the ebb tidal flow is remarkably hindered when compared to the flood tidal phase, resulting in an asymmetrical temporal pattern. The retention of the backwash current may provide a serene environment favorable for marine organisms and stagnation zones where suspended sediment tends to settle. However, water pollution or flood situations may also be exacerbated because of such a stagnation of seawater.

Figure 7 shows the tidal attenuation ratios that means to what percentage of an incident tidal amplitude is attenuated by the mangrove landfill. The attenuation ratio for the water depth of 30 cm and the width of 500 m is calculated 64% if the plant is fully grown. However, just 12% is expected when the construction of the landfill is finished. As confirmed by Equation (2), the bottom friction increases with the square of Manning's n value, and thus the growth ratio appears to be one of the important design parameters.

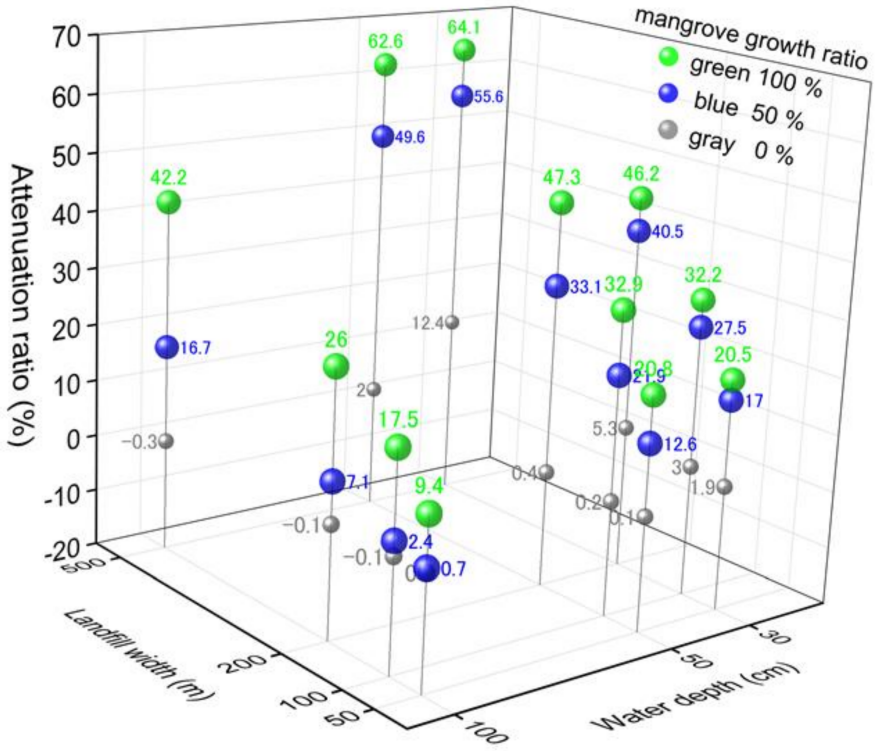

Figure 7. Tidal attenuation ratio, which differ with plant growth ratio, landfill width, and water depth.

Correlation and multiple regression analyses were conducted to examine the relationship between attenuation ratio and three potential predictors: landfill width, water depth, and growth ratio. Table 3 summarizes the analysis results. The multiple regression model demonstrates the significance of all three predictors on the attenuation which can be expressed as follows, with $R^2 = 0.802$, $F(3, 32) = 48.3$, $p < 0.001$.

Table 3. Regression coefficients and *p*-value of tide attenuation ratio.

	Coefficients	Std. Error	*t* Stat.	*p*-Value	Lower 95%	Upper 95%
intercept	7.824	4.210	1.858	0.072	−0.752	16.40
landfill width	0.051	0.008	6.051	9.36^{-7}	0.034	0.068
water depth	−0.249	0.050	−4.961	2.23^{-5}	−0.351	−0.147
growth ratio	0.331	0.036	9.147	19.1^{-10}	0.257	0.404

$$\text{Attenuation ratio [\%]} = 7.824 + 0.051 \times \text{landfill width [m]}$$
$$-0.249 \times \text{water depth [m]} + 0.331 \times \text{growth ratio [\%]} \quad (9)$$

Water depth is negatively correlated with the attenuation ratio, indicating that resistance from the bed becomes weaker as water depth becomes deeper. A direct comparison among the parameters with different dimensions and magnitudes may not make strong sense. However, this regression analysis suggests that water depth and growth ratio have the same order of contribution, while the landfill width is less influential.

3.2. Flow Characteristics

The velocity of the long-period wave u can be calculated by the formula: $u = A\sqrt{g/h}$, where A is wave amplitude, g is gravitational acceleration, and h is water depth [22]. Note that u is not a

function of vertical position; the horizontal velocity is uniform over depth. For example, the velocity is calculated at 1.3 m/s when a wave with the amplitude of 30 cm propagates the shallow water depth of 50 cm. The equation implies that the velocity increases as the water depth becomes shallow. Figure 8 also shows an increase in velocity when the tide reaches the landfill where the water depth is shallow. However, the velocity rapidly decreases as the tide propagates over the landfill due to increased flow resistance. The abovementioned theoretical formula inevitably overestimates velocities for such a shallow region. In the beginning stage of the mangrove landfill, the peak velocity reaches up to 12 cm/s. However, the maximum velocity is expected to become as small as a few cm/s after the plant fully grows.

By the way, the computational domain is partitioned into 600 elements with a length (Δx) of 50 m each, while the time increment (Δt) is selected 0.2 s (Table 2). Therefore, the maximum Courant number (=velocity $\times$ $\Delta t/\Delta x$ = 0.12 m/s $\times$ 0.2 s/50 m) is sufficiently smaller than unity, satisfying the CFL condition.

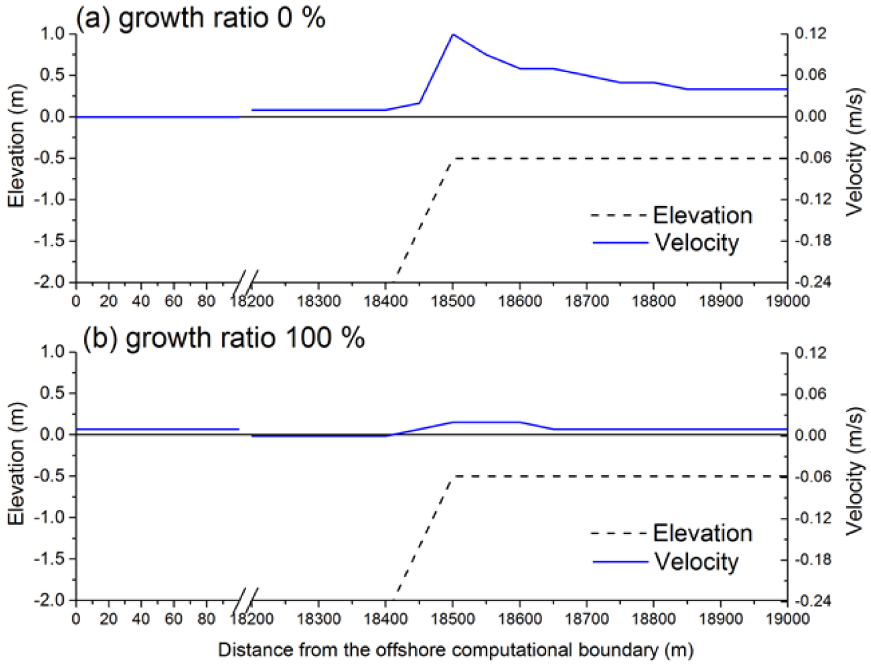

Figure 8. Profile of maximum flow-velocity during one tidal cycle. Note that the water depth was assumed to be 50 cm.

4. Discussion

As demonstrated in the previous section, the mangrove landfill cannot effectively reduce tides unless it is carefully designed in advance. An equilibrium state may be achieved if the mangrove landfill is balanced among factors such as sea-level rise, soil consolidation, sediment deposition, and vegetation growth. The following suggestions may help planners in designing mangrove landfills. If the system is appropriately designed, expensive maintenance work will not be required over the lifetime of the mangrove landfill.

4.1. Mangrove Landfill Must Be Sufficiently High to Avoid a Total Submersion

Mangroves naturally grow in an intertidal zone above mean sea level, which is exposed during low tide and inundated during high tide for about 30% or less of the time [53]. Therefore, the mangrove plantation is often advised to be implemented within the intertidal zone. This guideline may be valid for a natural environmental condition, but not always be successful when the plantation is implemented in an urban area that is subjected to rapid subsidence.

4.2. Narrow Mangrove Landfills May Not Be Effective

Long-period waves such as tides cannot be effectively attenuated on a narrow mangrove belt. A wider landfill will be thus required for a substantial reduction effect. Nevertheless, the available room for the landfill will be limited, particularly in the case of urban coastal areas with a dense population. A narrow mangrove landfill should not be overestimated as a tidal attenuator, though it may still effectively work as a countermeasure against wind waves.

4.3. Mangroves Retain Seawater, Creating Both Positive and Negative Influences

A mangrove landfill causes the retention of seawater during the ebb tidal phase. A serene water environment is an advantage for marine organisms and animals, fostering biodiversity. On the other hand, stagnant seawater inevitably exacerbates coastal flooding because the discharge of storm water into the sea will be blocked by such accumulated water. As a consequence, water pollution problems may also occur.

4.4. Enhancing Sediment Deposition

The transformation of a tidal flat into a mangrove forest needs to meet critical conditions such as a sufficient sediment supply and low tidal/wind-wave energy conditions. Sediment deposition is expected to be the only dependable source to achieve the equilibrium state of a mangrove landfill against relative sea-level rise. The sediment deposition will also enhance the vegetation growth by yielding a nutrient-rich substrate, and in turn the erosion of the landfill will further decrease because of the hydraulic energy dissipation by increased resistance. Therefore, how to promote sediment deposition should be critical for the successful design of a mangrove landfill. As soon as the local elevation of the platform reaches a height suitable for halophytic plant development, the surface is colonized by vegetation, which promotes sediment trapping during submersion periods and contributes organic material [54–57].

4.5. Fluctuations of Mean-Sea Level

A shallower water environment is beneficial in reducing tidal energy. As demonstrated in the previous section, tidal damping will be remarkable if water depth can be limited and is sufficiently low. However, the mean-sea level is not static at all, rather, it fluctuates over time because of multiple mechanisms. One such mechanism is ENSO (El Niño Southern Oscillation). The 18.6-year lunar nodal cycle is also not negligible [11]. Sea level oscillations induced by ENSO are larger than the recent trends of sea-level rise [58].

4.6. Diversity of Species

Although beyond the scope of the present study, the diversity of plants in the mangrove landfill will also be critical for creating a tranquil water environment under a balanced ecosystem, which may eventually reduce flood risks by increasing flow resistance in the mangrove forests. Thus, different species tend to prefer different surface elevations, nutrients, saline conditions, and inundation patterns and frequencies [59–61]. For example, in Jakarta, *Avicennia marina*, commonly known as white or gray mangrove, is predominant and particularly important to attenuate waves [62]. However, *Rhizophora* sp. is also suitable in the areas that are fully inundated [19].

5. Conclusions

Mangrove landfills may effectively act as natural-infrastructural attenuators against coastal hazards, including tidal floods. However, their performance is not sustainable for many years unless the platform is appropriately designed. This study investigates the function of mangrove landfills in reducing tidal amplitudes by using the coupled numerical model between long-period wave and soil consolidation. The proposed model is able to simulate tidal damping on a mangrove landfill.

The landfill will vary in surface elevation over time because of soil consolidation, sea-level rise, sediment deposition, and vegetation growth, among many others. A mangrove landfill constructed without considering long-term topographical transitions will be submerged under the relative sea-level rise, and no remarkable effect on tidal attenuation is expected. The amplitude does not remarkably decrease where the mangrove growth ratio is low and the water depth is relatively deep. Therefore, the mangrove landfill needs to be designed by considering not only the initial stage but also over its lifetime to avoid system failures in the end. For instance, the case analysis for Jakarta Bay suggests that if the landfill of 200 m is fully covered by mangroves and sustained as shallow as 50 cm deep, the reduction in tidal amplitude reaches 40 to 50%.

Acknowledgments: This research was financed by MEXT/JSPS KAKENHI (16KK0121) and the Environment Research and Technology Development Fund (S-14) of Ministry of the Environment, Japan.

Conflicts of Interest: The author declares no conflict of interest.

References

1. Takagi, H.; Mikami, T.; Fujii, D.; Esteban, M. Mangrove forest against dyke-break induced tsunami in rapidly subsiding coasts. *Nat. Hazards Earth Syst. Sci.* **2016**, *16*, 1629–1638. [CrossRef]
2. Vuik, V.; Jonkman, S.N.; Borsje, B.W.; Suzuki, T. Nature-based flood protection: The efficiency of vegetated foreshores for reducing wave loads on coastal dikes. *Coast. Eng.* **2016**, *116*, 42–56. [CrossRef]
3. Tang, J.; Shen, Y.; Causon, D.M.; Qian, L.; Mingham, C.G. Numerical study of periodic long wave run-up on a rigid vegetation sloping beach. *Coast. Eng.* **2017**, *121*, 158–166. [CrossRef]
4. Primavera, J.H.; Esteban, J.M.A. A review of mangrove rehabilitation in the Philippines: Successes, failures and future prospects. *Wetl. Ecol. Manag.* **2008**, *16*, 345–358. [CrossRef]
5. Alongi, D.M. Mangrove forests: Resilience, protection from tsunamis, and responses to global climate change. *Estuar. Coast. Shelf Sci.* **2008**, *76*, 1–13. [CrossRef]
6. Gunderson, L.H.; Holling, C.S.; Pritchard, L., Jr.; Peterson, G.D. Resilience of large-scale resource systems. In *Resilience and the Behaviour of Large-Scale Systems*; Gunderson, L.H., Pritchard, L., Jr., Eds.; Island Press: Washington, DC, USA, 2002.
7. Walker, B.; Holling, C.S.; Carpenter, S.R.; Kinzig, A. Resilience, adaptability and transformability in social–ecological systems. *Ecol. Soc.* **2004**, *9*, 9. [CrossRef]
8. Renaud, F.G.; Sudmeier-Rieux, K.; Estrella, M. The Role of Ecosystems in Disaster Risk Reduction, 2013. Available online: http://collections.unu.edu/view/UNU:1995 (accessed on 30 March 2018).
9. CNRD-PEDRR Disasters. *Environment and Risk Reduction—Eco-DRR Master's Module, Instructor's Manual*; Center for Natural Resources and Development, Partnership on Environment and Disaster Risk Reduction: Kenya, 2013; 102p, Available online: https://www.preventionweb.net/educational/view/54583 (accessed on 30 March 2018).
10. Dosewald, N.; Estrella, M. *Promoting Ecosystems for Disaster Risk Reduction and Climate Change Adaptation*; Discussion Paper; UNEP: Geneva, Switzerland, 2015; 52p, Available online: http://postconflict.unep.ch/publications/Eco-DRR/Eco-DRR_Discussion_paper_2015.pdf (accessed on 30 March 2018).
11. Takagi, H.; Esteban, M.; Mikami, T.; Fujii, D. Projection of coastal floods in 2050 Jakarta. *Urban Clim.* **2016**, *17*, 135–145. [CrossRef]
12. Takagi, H.; Fujii, D.; Esteban, M.; Yi, X. Effectiveness and Limitation of Coastal Dykes in Jakarta: The Need for Prioritizing Actions against Land Subsidence. *Sustainability* **2017**, *9*, 619. [CrossRef]
13. Jamero, M.L.; Onuki, M.; Esteban, M.; Billones-Sensano, X.K.; Tan, N.; Nellas, A.; Takagi, H.; Thao, N.D.; Valenzuela, V.P. Small-island communities in the Philippines prefer local measures to relocation in response to sea-level rise. *Nat. Clim. Chang.* **2017**, *7*, 581–586. [CrossRef]
14. Giosan, L.; Syvitski, J.; Constantinescu, S.; Day, J. Protect the world's deltas. *Nature* **2014**, *516*, 31–33. [CrossRef] [PubMed]
15. Takagi, H.; Thao, N.D.; Anh, L.T. Sea-level rise and land subsidence: Impacts on flood projections for the Mekong delta's largest city. *Sustainability* **2016**, *8*, 959. [CrossRef]
16. Krauss, K.W.; McKee, K.L.; Lovelock, C.E.; Cahoon, D.R.; Saintilan, N.; Reef, R.; Chen, L. How mangrove forests adjust to rising sea level. *New Phytol.* **2014**, *202*, 19–34. [CrossRef] [PubMed]

17. Lovelock, C.E.; Cahoon, D.R.; Friess, D.A.; Guntenspergen, G.R.; Krauss, K.W.; Reef, R.; Rogers, K.; Saunders, M.L.; Sidik, F.; Swales, A.; et al. The vulnerability of Indo-Pacific mangrove forests to sea-level rise. *Nature* **2015**, *526*, 559–563. [CrossRef] [PubMed]
18. Sasmito, S.D.; Murdiyarso, D.; Friess, D.A.; Kurnianto, S. Can mangroves keep pace with contemporary sea level rise? A global data review. *Wetl. Ecol. Manag.* **2016**, *24*, 263–278. [CrossRef]
19. Oka, S.; Orishimo, S.; Nagano, A. Natural symbiosis type fishing port rehabilitation using the mangrove (example of the Jakarta fishing port). *JSCE Proc. Civ. Eng. Ocean* **2004**, *20*, 1151–1156. [CrossRef]
20. Munk, W.H. Origin and Generation of Waves. In Proceedings of the First Conference on Coastal Engineering, Long Beach, CA, USA, October 1950; Available online: https://journals.tdl.org/icce/index.php/icce/article/view/904 (accessed on 30 March 2018).
21. Kowalik, Z.; Murty, T.S. *Numerical Modeling of Ocean Dynamics*; World Scientific: Singapore, 1993; p. 481.
22. Battjes, J.; Labeur, R.J. *Unsteady Flow in Open Channels*; Cambridge University Press: Cambridge, UK, 2017; p. 299.
23. Horvath, Z.; Waser, J.; Perdigao, R.A.P.; Konev, A.; Bloschl, G. A Two-Dimensional Numerical Scheme of Dry/Wet Fronts for the Saint-Venant System of Shallow Water Equations. *Int. J. Numer. Meth. Fluids* **2015**, *77*, 159–182. [CrossRef]
24. Dean, R.G.; Dalrymple, R.A. *Water Wave Mechanics for Engineers and Scientists*; World Scientific Publishing: Singapore, 1984; p. 371.
25. Roeber, V.; Bricker, J.D. Destructive tsunami-like wave generated by surf beat over a coral reef during Typhoon Haiyan. *Nat. Commun.* **2015**, *6*, 7854. [CrossRef] [PubMed]
26. Wesley, L.D. *Fundamentals of Soil Mechanics for Sedimentary and Residual Soils*; Wiley: Hoboken, NJ, USA, 2010; p. 431.
27. Knappett, J.A.; Craig, R.F. *Craig's Soil Mechanics Eighth Edition*; CRC Press: Boca Raton, FL, USA, 2011; p. 552.
28. Osterberg, J.O. Influence values for vertical stresses in a semi infinite mass due to an embankment loading. In Proceedings of the Fourth International Conference on Soil Mechanics and Foundation Engineering, London, UK, 12–24 August 1957; Volume 1, pp. 393–394.
29. Einstein, H.A. The Bedload Function for Sediment Transportation in Open Channel Flows. Soil Conservation Service U.S. Department Agriculture Technical Bulletin No. 1026. 1950, p. 78. Available online: http://xon.sdsu.edu/einstein_bedload_function.pdf (accessed on 30 March 2018).
30. Bagnold, R.A. Mechanics of marine sedimentation. In *The Sea*; Hill, M.N., Ed.; Wiley: New York, NY, USA, 1963; pp. 507–582.
31. Dean, R.G. *Beach Nourishment: Theory and Practice*; World Scientific: Singapore, 2002.
32. Heathershaw, A.D. Comparisons of measured and predicted sediment transport rates in tidal currents. *Mar. Geol.* **1981**, *42*, 75–104. [CrossRef]
33. Furukawa, K.; Wolanski, E. Sedimentation in mangrove forests. *Mangroves Salt Marshes* **1996**, *1*, 3–10. [CrossRef]
34. Green, J.C. Modelling flow resistance in vegetated streams: Review and development of new theory. *Hydrol. Processes* **2005**, *19*, 1245–1259. [CrossRef]
35. Mazda, Y.; Wolanski, E.; King, B.; Sase, A.; Ohtsuka, D.; Magi, M. Drag force due to vegetation in mangrove swamps. *Mangroves Salt Marshes* **1997**, *1*, 193–199. [CrossRef]
36. Maza, M.; Lara, J.L.; Losada, I.J. Tsunami wave interaction with mangrove forests: A 3-D numerical approach. *Coast. Eng.* **2015**, *98*, 33–54. [CrossRef]
37. Losada, I.J.; Maza, M.; Lara, J.L. A new formulation for vegetation-induced damping under combined waves and currents. *Coast. Eng.* **2016**, *107*, 1–13. [CrossRef]
38. Bricker, J.D.; Gibson, S.; Takagi, H.; Imamura, F. On the need for larger Manning's roughness coefficients in depth-integrated tsunami inundation models. *Coast. Eng. J.* **2015**, *57*, 13. [CrossRef]
39. Wolanski, E.; Jones, M.; Bunt, J.S. Hydrodynamics of a tidal creek-mangrove swamp system. *Aust. J. Mar. Freshwater Res.* **1980**, *31*, 431–450. [CrossRef]
40. Arcement, G.J., Jr.; Schneider, V.R. *Guide for Selecting Manning's Roughness Coefficients for Natural Channels and Flood Plains*; Report No. FHWA-TS-84-204; Federal Highway Administration: Washington, DC, US, 1984.
41. Furukawa, K.; Wolanski, E.; Mueller, H. Currents and sediment transport in mangrove forests. *Estuar. Coast. Shelf Sci.* **1997**, *44*, 301–310. [CrossRef]

42. Xu, H.; Zhang, K.; Shen, J.; Li, Y. Storm surge simulation along the U.S. East and Gulf Coasts using a multi-scale numerical model approach. *Ocean Dyn.* **2010**, *60*, 1597–1619. [CrossRef]
43. Diaz, R.G. Analysis of Manning coefficient for small-depth flows on vegetated beds. *Hydrol. Process.* **2005**, *19*, 3221–3233. [CrossRef]
44. Perillo, G.M.E.; Wolanski, E.; Cahoon, D.R.; Brinson, M.M. *Coastal Wetlands: An Integrated Ecosystem Approach*; Elsevier: Amsterdam, The Netherlands, 2009.
45. Lynch, J.C.; Meriwether, J.R.; McKee, B.A.; Vera-Herrera, F.; Twilley, R.R. Recent accretion in mangrove ecosystems based on 137Cs and 210Pb. *Estuaries* **1989**, *12*, 284–299. [CrossRef]
46. Day, J.W.; Templet, P.H. Consequences of sea level rise: Implication from the Mississippi Delta. *Coast. Manag.* **1989**, *17*, 241–257. [CrossRef]
47. Wood, M.E.; Kelley, J.T.; Belknap, D.F. Patterns of sediment accumulation in the tidal marshes of Maine. *Estuaries* **1989**, *12*, 237–246. [CrossRef]
48. Kearney, M.S.; Stevenson, J.C.; Ward, L.G. Spatial and temporal changes in marsh vertical accretion rates at Monie Bay: Implication for sea-level rise. *J. Coast. Res.* **1994**, *10*, 1010–1020.
49. Parkinson, R.W.; DeLaune, R.D.; White, J.R. Holocene sea-level rise and the fate of mangrove forests within the wider Caribbean region. *J. Coast. Res.* **1994**, *10*, 1077–1086.
50. Blum, L.K.; Christian, R.R. Belowground production and decomposition along a tidal gradient in a Virginia salt marsh. In *The Ecogeomorphology of Salt Marshes*; American Geophysical Union: Washington, DC, USA, 2004; pp. 47–74.
51. Saad, S.; Husain, M.L.; Yaacob, R.; Asano, T. Sediment accretion and variability of sedimentological characteristics of a tropical estuarine mangrove: Kemaman, Terengganu, Malaysia. *Mangroves Salt Marshes* **1999**, *3*, 51–58. [CrossRef]
52. Woodroffe, C. Mangrove sediments and geomorphology. In *Tropical Mangrove Ecosystem*; Robertson, A.I., Alongi, D.M., Eds.; American Geophysical Union: Washington, DC, USA, 1992; pp. 7–41.
53. Lewis, R.R. Ecological engineering for successful management and restoration of mangrove forests. *Ecol. Eng.* **2005**, *24*, 403–418. [CrossRef]
54. Leonard, L.; Luther, M. Flow hydrodynamics in tidal marsh canopies. *Limnol. Oceanogr.* **1995**, *40*, 1474–1484. [CrossRef]
55. Christiansen, T.; Wiberg, P.L.; Milligan, T.G. Flow and sediment transport on a tidal salt marsh surface. *Estuar. Coast. Shelf Sci.* **2000**, *50*, 315–331. [CrossRef]
56. Morris, J.T.; Sundareshwar, P.V.; Nietch, C.T.; Kjerfve, B.; Cahoon, D.R. Responses of coastal wetlands to rising sea level. *Ecology* **2002**, *83*, 2869–2877. [CrossRef]
57. D'Alpaos, A.; Lanzoni, S.; Rinaldo, A.; Marani, M. Chapter 5: Coastal wetlands: A synthesis. In *Coastal Wetlands: An Integrated Ecosystem Approach*; Perillo, G.M.E., Wolanski, E., Cahoon, D.R., Brinson, M.M., Eds.; Elsevier: Amsterdam, The Netherlands, 2009; pp. 159–184.
58. Losada, I.J.; Reguero, B.G.; Mendez, F.J.; Castanedo, S.; Abascal, A.J.; Minguez, R. Long-term changes in sea-level components in Latin America and the Caribbean. *Glob. Planet. Chang.* **2013**, *104*, 34–50. [CrossRef]
59. Global Nature Fund. *Global Nature Fund Mangrove Rehabilitation Guidebook*; GNF: Radolfzell, Germany, 2007; p. 69.
60. Wolanski, E.; Brinson, M.M.; Cahoon, D.R.; Perillo, G.M.E. Chapter 1: Coastal wetlands: A synthesis. In *Coastal Wetlands: An Integrated Ecosystem Approach*; Perillo, G.M.E., Wolanski, E., Cahoon, D.R., Brinson, M.M., Eds.; Elsevier: Amsterdam, The Netherlands, 2009; pp. 1–62.
61. Sarker, S.K.; Reeve, R.; Thompson, J.; Paul, N.K.; Mattiopoulos, J. Are we failing to protect threatened mangroves in the Sundarbans world heritage ecosystem? *Sci. Rep.* **2016**, *6*, 21234. [CrossRef] [PubMed]
62. Herison, A.; Yulianda, F.; Kusmana, C.; Nurjaya, I.W.; Adrianto, L. The Existing Condition of Mangrove Region of Avicennia marina: Its Distribution and Functional Transformation. *JMHT* **2014**, *20*, 26–34. [CrossRef]